JOURNAL OF AIRCRAFT
Vol. 47, No. 3, May–June 2010

Engineering Notes

Preliminary Experimental Investigation of a Morphable Biplane: The X-Wing

Lance W. Traub,* Robert Snyder,† and Thomas Pellino†
Embry-Riddle Aeronautical University, Prescott, Arizona 86301

DOI: 10.2514/1.46322

Nomenclature

AR	=	aspect ratio
b	=	wing span
C_{Dv}	=	vortex drag coefficient
C_L	=	lift coefficient
$C_{L\alpha}$	=	lift-curve slope
C_{Lmd}	=	lift coefficient for minimum drag
D	=	drag
e	=	inviscid span efficiency factor
h	=	height or gap, see Eq. (11)
L	=	lift
m_{22}	=	apparent mass per unit length
q	=	dynamic pressure
$\underline{S_{\mathrm{mono}}}$	=	area of influence of the apparent mass for the reference monoplane
S_{mono}	=	monoplane reference area
U	=	freestream velocity
x	=	coordinate
α	=	angle of attack
γ	=	nonplanarity parameter, see Eq. (2)
ρ	=	density
ϕ	=	anhedral/dihedral angle
Ψ	=	apparent mass increase for conventional biplane, see Eq. (6)

Subscripts

mono	=	monoplane
max	=	maximum
X-wing	=	pertaining to X-wing configuration

Introduction

THE promise of enhanced performance and mission capability, motivated by the flexibility demonstrated by avian flyers, has promulgated a serious and focused research effort to develop morphing technology. While not new as a concept (swing wings), recent efforts have focused on significant geometry or configuration changes [1,2]. Aircraft that may benefit significantly from morphing technology would be unmanned aerial vehicles (UAVs). Their greater simplicity of design and lack of complication from omission of the human component promotes enhanced ability to incorporate advanced technology. Current planform-changing technology is evidenced by NextGen's interpretation of variable sweep and Lockheed's variable-span wing [3,4]. Most small UAVs or micro UAVs generally have comparatively low-AR wings. This aids in increasing the sectional Reynolds number Re, increases structural rigidity, and reduces sensitivity to atmospheric turbulence. However, a byproduct is comparatively poor lifting ability, exacerbated by the low-Reynolds-number environment (often in the 100,000 to 200,000 range).

The benefits of wing nonplanarity for a constrained wing span are well known and include enhanced lift and reduced inviscid lift-dependent drag. Studies have indicated that nonplanarity is most effective near the wing tips [5] (i.e., end plates). For a multiwing interpretation of nonplanarity, the increase in zero-lift drag and structural weight usually overshadows any realizable benefit. For a small UAV-type vehicle, often designed for observation, the ability to maximize range and endurance coupled with a high dash speed to get on target quickly would be valuable. Unfortunately, the operating environment and geometric constraints are at odds with this requirement. Consequently, an obvious design space would be that for a flight vehicle that could morph from a monoplane (dash) to biplane (endurance and potentially range). Consideration of geometry would mitigate against morphing a monoplane directly to a biplane by having a vertically movable upper or lower wing. The required mechanism (probably a scissor jack derivative) would be bulky and heavy. An obvious solution is a biplane that morphs from a monoplane to a configuration resembling an X-wing. This could be accomplished by rotating the wings (instead of translating them), resulting in a vastly simpler structure. Additionally, the efficiency loss for a given wing-tip height to semispan, compared with a regular biplane, is small [6].

Consequently, in this Note, an experimental investigation is described that evaluates the possibility of performance benefits for a generic X-wing design. The envisaged concept is for the wings (or a cylindrical body section on which they are attached) to rotate to transform from monoplane to biplane. This requires the wings to be able to merge to form the monoplane. As a result, a wing section may be required with a flexible skin to accommodate merging, or a thin wing section such as a flat plate or circular arc would be needed. A theoretical method is developed to estimate the lift and vortex drag and is compared with numerical estimates and experiment.

Equipment and Procedure

Wind-tunnel tests were conducted in Embry-Riddle University's 1 by 1 ft open-return facility. This wind tunnel has a measured turbulence intensity of 0.5% and jet uniformity within 1% in the core. The wall boundary layer is approximately 5 mm thick. Force measurements were taken using an in-house-designed and in-house-manufactured low-range platform balance. The balance has a maximum range of 43 N and a demonstrated accuracy, resolution, and repeatability of 0.0098 N. Angle-setting ability is within 0.1 deg. A computer-controlled acquisition system was written for this balance using LabVIEW 8.2. A generic reflection-plane X-wing model was rapid-prototyped in ABS (acrylonitrile butadiene styrene) plastic, as shown in Fig. 1a. Wind-tunnel model installation is shown in Fig. 1b. The gap between the fuselage half-body and wind-tunnel wall was approximately 0.5 mm. The model used a 3.37%-thick, 5%-camber circular arc airfoil (formed into a rectangular wing), as this airfoil is effective at low Reynolds numbers and is conducive for wing merging. The symmetrical monoplane ($\phi = 0$ deg) AR was 3.63, formed with a semispan ($b/2$) of 0.127 m and a chord of 0.07 m. A hemisphere cylinder half-body was used to accommodate wing attachment. Wing anhedral/dihedral angles of 5 to 45 deg were

Received 13 July 2009; revision received 14 January 2010; accepted for publication 20 January 2010.

*Associate Professor, Aerospace and Mechanical Engineering Department. Member AIAA.
†Undergraduate Student, Aerospace and Mechanical Engineering Department.

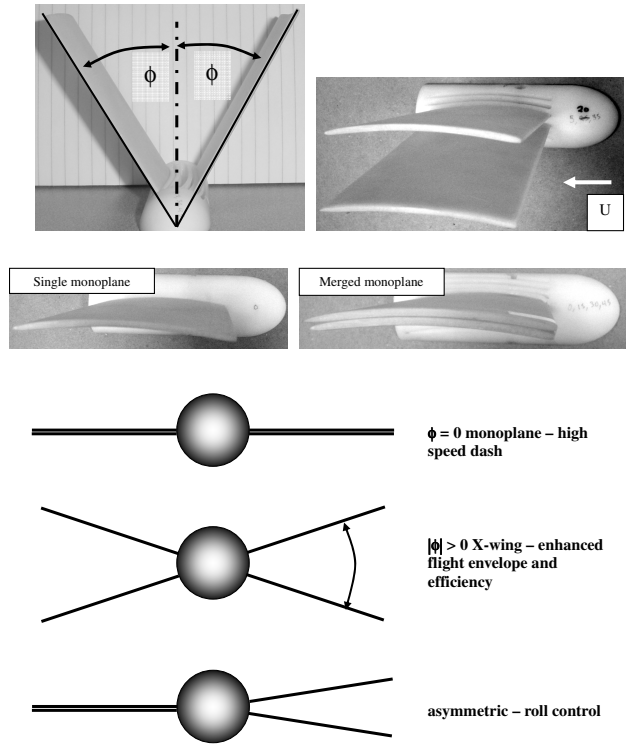

a)

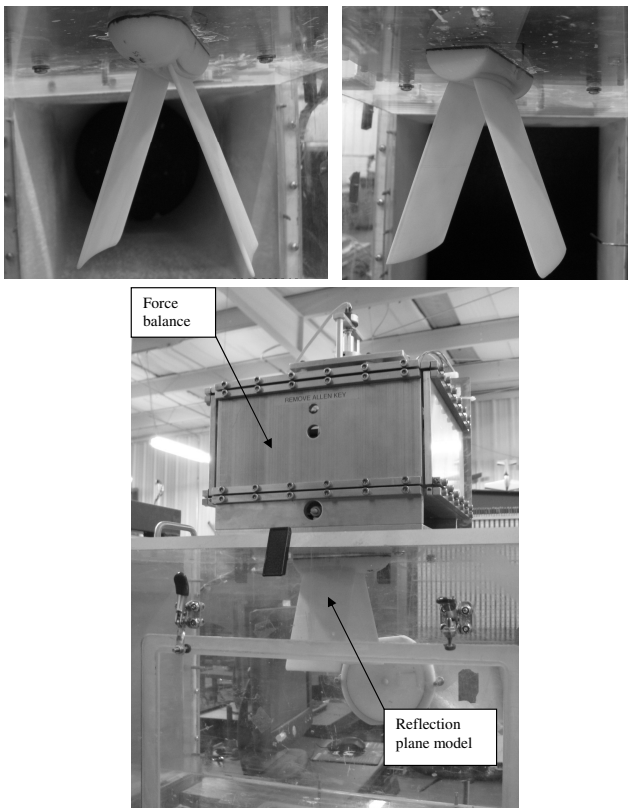

b)

Fig. 1 X-wing a) configuration settings and wind-tunnel model and b) installation.

evaluated. The wings were located by insertion into suitably angled slots in the body. For any nonplanar test, the anhedral and dihedral angles were set to be equal. Note that the projected wing span reduces with ϕ, as wing span was not constrained; the same wings were used for all tests. All coefficients were referred to the monoplane area ($\phi = 0$ deg). Thus, the data directly show the performance improvement or decrement when nonplanarity is employed. Two monoplane configurations are included for reference: one formed from a single wing (designated as single) and the other formed from merging the two wings (designated as double) (see Fig. 1). Wall corrections were not applied to the data, due to the model configuration, mounting style, and comparative nature of the tests.

Theory Development

It would be valuable for conceptual or preliminary design purposes to have an analytic expression to estimate the potential performance of an X-wing configuration. An added benefit of a predictive equation is its ability to explicitly show the variable dependencies. The approach adopted to analyze the wings follows from slender-wing theory, where the flow is analyzed in a crossflow plane. Force coefficients are determined from the streamwise change of the apparent mass per unit length (m_{22}) associated with the cross section. A necessary requirement using this approach is to determine the effect of wing anhedral/dihedral on the apparent mass. To establish this, the wing rotation is decomposed into two effects. The first is an isolated V-wing and the second is a conventional biplane. The X-wing is analyzed as if constituted of both of these effects. To analyze the V-wing, the apparent mass formulation from Letcher [7] will be used. The following derivation references all expressions to the area of the monoplane, i.e., the wing with no anhedral/dihedral. The lift per unit length of the wing is given by

$$\frac{\mathrm{d}L}{\mathrm{d}x} = U^2 \alpha \frac{\mathrm{d}m_{22}}{\mathrm{d}x} \tag{1}$$

Following Letcher [7], Smith [8], and Lowson [5], the apparent mass of a V-wing may be expressed as

$$m_{22} = \rho \underline{S_{\text{mono}}(x)} \left(\frac{1-\gamma}{\gamma}\right)^{(2\gamma-1)} \quad \text{with} \quad \gamma = \frac{\pi/2 - \phi}{\pi} \tag{2}$$

where the expression is based on the reference area of the wing with no dihedral, i.e., flat, and $\underline{S_{\text{mono}}(x)}$ is the area of influence of the apparent mass for this reference monoplane, i.e., $\pi b(x)^2/4$. This expression was derived in the Trefftz plane, a crossflow plane located at downstream infinity. Thus, effects of anhedral and dihedral are similar to the effects of the bound, and trailing vortices on the wing's vortex system are neglected. The wing lift is

$$L = \int_0^x \frac{\mathrm{d}L}{\mathrm{d}x}\,\mathrm{d}x \tag{3}$$

Substitution of Eqs. (1) and (2) and $\underline{S_{\text{mono}}}(x) = \pi b(x)^2/4$ into Eq. (3) yields

$$L = U^2 \alpha \rho \underline{S_{\text{mono}}} \left(\frac{1-\gamma}{\gamma}\right)^{(2\gamma-1)} \tag{4}$$

where $\underline{S_{\text{mono}}}$ is then given by $\pi b^2/4$. Nondimensionalizing by the dynamic pressure and monoplane reference area yields a lift-curve slope for the V-wing of

$$C_{L\alpha\text{V-wing}} = \frac{L}{qS_{\text{mono}}\alpha} = \frac{2\underline{S_{\text{mono}}}}{S_{\text{mono}}} \left(\frac{1-\gamma}{\gamma}\right)^{(2\gamma-1)} \tag{5}$$

The effect of having an X-wing constituted of a merged $\bigvee$ and $\bigwedge$ wing section will be treated as a conventional biplane effect; i.e., increasing the dihedral/anhedral angle between the wings has an analogous effect to increasing the gap of a biplane. Thus, the apparent mass area of influence of the of the X-wing may be written as (where ψ relates to the increase of apparent mass for a conventional biplane)

$$\underline{S_{\text{X-wing}}} = \underline{S_{\text{mono}}}\Psi \tag{6}$$

Substitution of Eq. (6) into Eq. (5) with $\underline{S_{\text{mono}}} = \pi b^2/4$ yields an expression for the lift curve of the X-wing as

$$C_{L\alpha\text{X-wing}} = \frac{2\pi b^2 \Psi}{4S_{\text{mono}}}\left(\frac{1-\gamma}{\gamma}\right)^{(2\gamma-1)} \tag{7}$$

which simplifies to (AR_{mono} is the monoplane aspect ratio, i.e., $\phi = 0$ deg)

$$C_{L\alpha\text{X-wing}} = \left(\frac{\pi \text{AR}_{\text{mono}}}{2}\right)\Psi\left(\frac{1-\gamma}{\gamma}\right)^{(2\gamma-1)} \tag{8}$$

The first term in brackets on the right-hand side is seen to be the lift-curve slope for a slender delta wing, as given by Jones [9]. Consequently, this term may be interpreted and rewritten as a lift-curve slope: in this presentation, that of the monoplane (X-wing with 0 deg anhedral/dihedral). Thus, we may write

$$C_{L\alpha\text{X-wing}} = C_{L\alpha\text{-mono}}\Psi\left(\frac{1-\gamma}{\gamma}\right)^{(2\gamma-1)} \tag{9}$$

This expression decomposes the lift of the X-wing into a monoplane lift-curve slope ($C_{L\alpha\text{-mono}}$) multiplied by two terms that account for the effect of a single V-wing configuration on the apparent mass in conjunction with a biplane effect Ψ. An expression for Ψ is required. Munk [10] presents tables for the apparent mass of a biplane as a function of gap h referenced to that of a monoplane (i.e., $/\pi b^2/4$), which may be fitted with a polynomial regression to result in

$$\Psi = -3.195\left(\frac{h}{b_{\text{mono}}}\right)^6 + 12.991\left(\frac{h}{b_{\text{mono}}}\right)^5 - 20.205\left(\frac{h}{b_{\text{mono}}}\right)^4 + 15.621\left(\frac{h}{b_{\text{mono}}}\right)^3 - 7.07\left(\frac{h}{b_{\text{mono}}}\right)^2 + 2.694\left(\frac{h}{b_{\text{mono}}}\right) + 1 \tag{10}$$

A complication is in the definition of h, as the effective height of the biplane for a given X-wing anhedral/dihedral is not clear. A relation may be established from consideration of the Trefftz plane wake trace (a circle of diameter b_{mono}). If the trace is divided in half along a vertical line, the vertical displacement of the centroids [$h = 2[2b/2\pi]\sin(\phi)$] for each half (two wings per side) may be considered as the effective biplane gap for a set anhedral/dihedral. Dividing h by the projected semispan of the V-wing ($\cos(\phi)b/2$) results in

$$\frac{h}{b_{\text{mono}}} = \frac{4\tan(\phi)}{\pi} \tag{11}$$

Note that although the semispan is used in the derivation, consideration of the V-wing geometry suggests that this should be used as the equivalent b_{mono} in Eq. (10).

Following Letcher [7], the vortex drag of the wing, C_{Dv}. may be estimated from (after generalizing to accommodate cambered airfoil sections)

$$C_{Dv} = \frac{1}{4}\left(\frac{\rho S_{\text{mono}}}{m_{22}}\right)(C_L - C_{\text{Lmd}})^2 \tag{12}$$

Simplification upon substitution of Eqs. (2) and (6) yields

$$C_{Dv} = \frac{1}{\pi \text{AR}_{\text{mono}}\Psi}\left(\frac{1-\gamma}{\gamma}\right)^{(1-2\gamma)}(C_L - C_{\text{Lmd}})^2 \tag{13}$$

The impact of X-wing dihedral on the inviscid span efficiency factor e may be estimated by equating Eq. (13) to $C_{Dv} = (C_L - C_{\text{Lmd}})^2/(\pi \text{AR}_{\text{mono}} e)$, which yields

$$e = \Psi\left(\frac{1-\gamma}{\gamma}\right)^{(2\gamma-1)} \tag{14}$$

Examination of Eq. (14) shows that the span efficiency for the wings relates directly to the change of lift-curve slope with nonplanarity [see Eq. (9)]. Equations (9–11) and (14) may be used to estimate the impact of an X-wing configuration. The lift-curve slope of the monoplane (the closed X-wing) may be estimated from experiment or any suitable theory or numerical method.

Results and Discussion

Figures 2 and 3 present experimentally measured effects of nonplanarity on the lift and drag coefficients and L/D for $Re = 80,000$ and 125,000. Increasing ϕ is seen to significantly increase the lift-curve slope and maximum lift. The incremental effect of ϕ reduces rapidly for $\phi > 10$ deg. The merged monoplane wing (designated as double) shows a performance loss compared with the monoplane wing formed using only one wing (single, included for reference). For larger ϕ (greater than 30 deg), performance is seen to degrade (symbols are in gray to aid observation). Consequently, efficiency gains through nonplanarity are outweighed by the loss of projected lifting area. A similar result is noted at $Re = 125,000$ (Fig. 3). Observe that all configurations show a large maximum-lift plateau, without any significant loss after maximum lift is achieved for the tested incidence range. The drag polar shows a significant minimum-drag increase, as the wetted area essentially doubles for $\phi > 0$ deg, compared with the single monoplane. This may be examined clearly in Fig. 2, in which the minimum-drag region has been enlarged. It may also be seen that the merged monoplane also shows an increase in minimum drag compared with the single monoplane. As observed for lift, drag systematically decreases as ϕ increases until approximately 30 deg, beyond which performance starts to degrade for both $Re = 80,000$ and 125,000 (Figs. 2 and 3). Nonplanarity shows a significant improvement in recorded L/D performance for lift coefficients greater than 0.7, compared with the single monoplane; not only does $(L/D)_{\max}$ increase for some ϕ

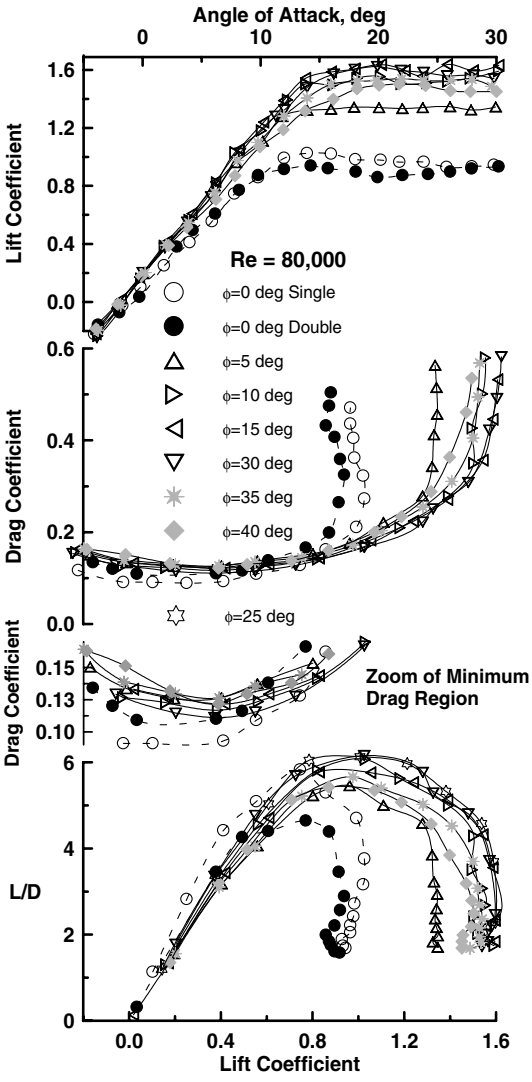

Fig. 2 Effect of nonplanarity on measured lift, drag, and L/D ratio; $Re = 80,000$.

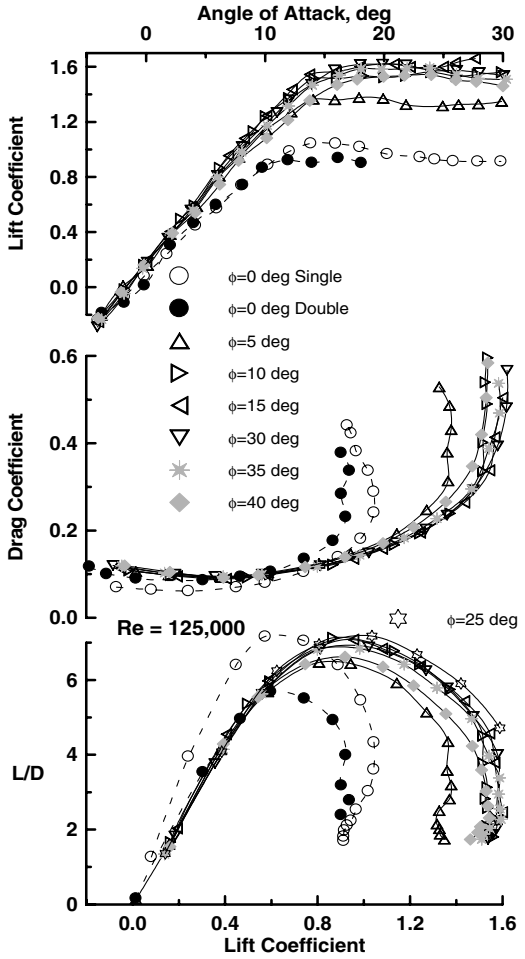

Fig. 3 Effect of nonplanarity on measured lift, drag, and L/D ratio; $Re = 125,000$.

settings, but the lift range over which near-maximum L/D is achieved is greatly expanded. This would greatly increase the flight envelope over which range can be maximized (allowing flexibility in the set flight speed for a given weight and altitude to achieve near-maximum range). Note that the merged monoplane shows a significant reduction in L/D compared with the single monoplane, primarily due to the drag penalty of this configuration. For $Re = 125,000$, the minimum-drag penalty degrades L/D of all X-wing configurations, compared with the single monoplane for C_L less than 0.7. A similar effect is noted for $Re = 80,000$ (Fig. 2) but is not as marked. Note that for $Re = 125,000$, a significant L/D plateau is still evident (Fig. 3), although its sustained extent is reduced compared with $Re = 80,000$. To gain insight into potential loiter enhancement for the X-wing, the endurance parameter $C_L^{3/2}/C_D$ is presented in Fig. 4. As indicated, this parameter increases markedly compared with the monoplane at high loading, suggesting potential improvements in vehicle endurance. To quantify the enhancement, $C_L^{3/2}/C_D$ and e were calculated for a representative case: $\phi = 25$ deg for $Re = 125,000$, giving $C_L^{3/2}/C_D = 7.79$ ($\phi = 20$ and 30 deg gave 7.69 and 7.55, respectively) and $e = 0.77$. The values for the single monoplane were $C_L^{3/2}/C_D = 6.06$ and $e = 0.466$, showing an increase in endurance of 29% for the X-wing. The double monoplane recorded $C_L^{3/2}/C_D = 4.74$. The present results show a significant reduction in performance when the wings merge to form the monoplane. For implementation, further investigation would be needed to find airfoil sections that can be effectively merged with minimal performance loss. An additional consideration for application would be to weigh the aerodynamic benefits of performance improvement against the likely increase in structural weight and complexity of the X-wing geometry.

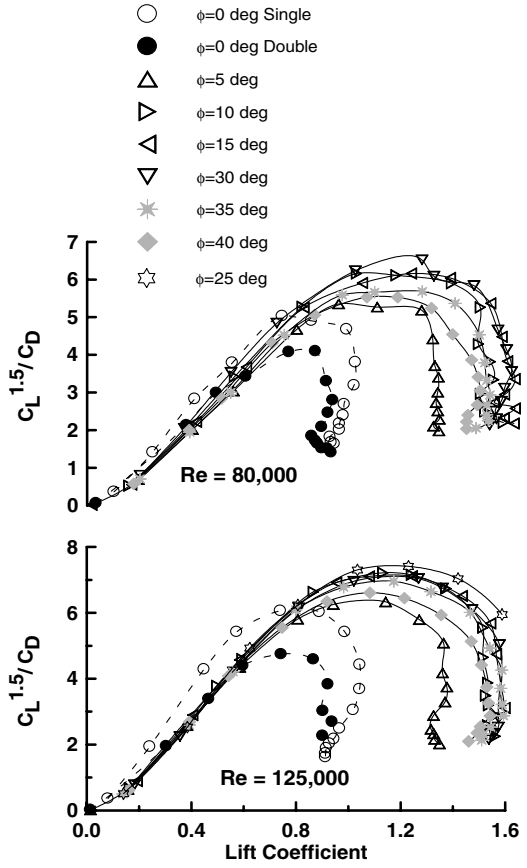

Fig. 4 Effect of nonplanarity on measured endurance parameter.

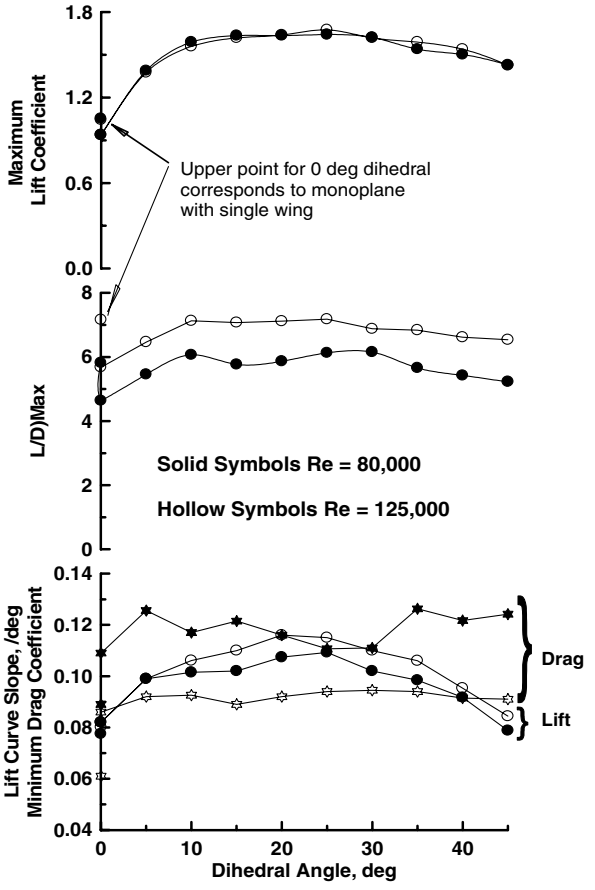

Fig. 5 Data summary showing effect of nonplanarity on measured longitudinal force coefficients.

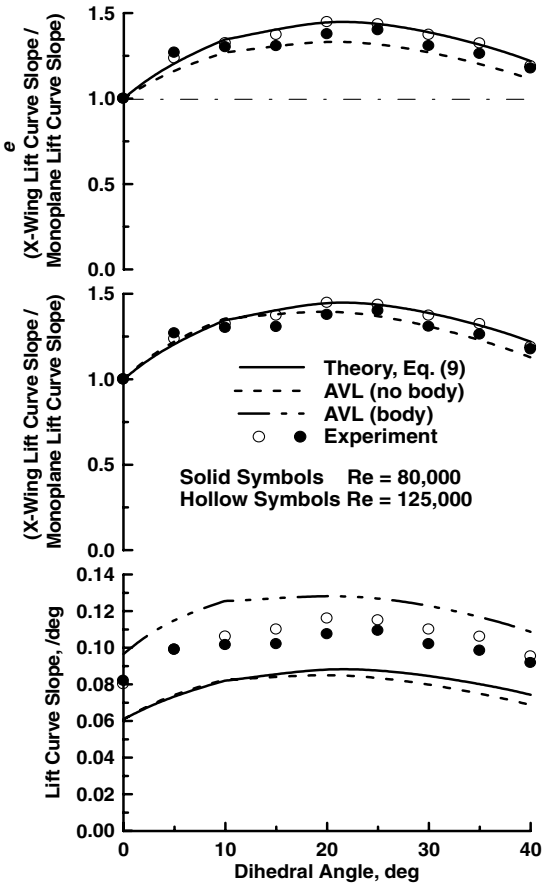

Fig. 6 Comparison of present method with experiment and numerical prediction.

Salient experimental performance parameters are summarized in Fig. 5. As may be seen, initial nonplanarity ($\phi = 5$ deg in these tests) shows a significant increase in wing lift-curve slope, $(L/D)_{\max}$ and maximum-lift coefficient, compared with either monoplane wing. These parameters peak for $20 \leq \phi \leq 30$ deg and then decline. Reynolds number effects are apparent on the lift-curve slope and L/D, but show little impact on the measured maximum lift for the Reynolds number range tested. The minimum-drag increment shows little variation once the wings deploy for $Re = 125,000$, but sensitivity to ϕ is apparent at the lower Reynolds numbers.

Looking at the present results does not show a clear benefit for using a morphable wing design. If endurance is the driving design goal, then a fixed X-wing configuration with $\phi = 25$ or 30 deg may be optimal (at least for the configuration explored in this study). However, if dash speed is also a design driver, then the weight penalty of the required morphing structure may be acceptable. To explore this, estimates of the maximum flight speed were made for a generic small UAV of the geometry used in this study. Experimental results for e and the minimum-drag coefficient were used. At maximum speed, the aircraft's thrust and drag are equal, allowing simple estimation of the maximum flight speed for steady level flight [11]. A fixed thrust of 2.5 N was selected, in conjunction with vehicle weights ranging from 5 to 10 N. Note that these values are essentially arbitrary and were selected for demonstration purposes. Calculation shows that with the assumption of equal weight for the single monoplane and the X-wing, the X-wing's maximum flight speed reduces by 19.3 and 18.2% compared with the monoplane, as the UAVs weight is set to 5 and 10 N. Assuming a weight increase of 25% for the X-wing vehicle over the monoplane shows a 20% reduction in maximum flight speed (monoplane and X-wing weighing 5 and 6.25 N, respectively) and 22% for a weight increase of 50% (monoplane and X-wing weighing 5 and 7.5 N, respectively). These calculations demonstrate that the X-wing's large minimum drag increase significantly reduces the maximum flight speed for a given installed thrust. Additionally, the increase in weight of the X-wing airframe would necessitate an increase in the fuel fraction for endurance increases to be dictated solely by the increment in $C_L^{3/2}/C_D$. Thus, the 25 and 50% weight increases cited for demonstration would incorporate both additional airframe weight and extra fuel. Consequently, if long loiter and high dash speeds are requirements, the variable-wing-geometry configuration may represent an effective design solution.

Figure 6 displays comparisons of the present theory [Eq. (9)] and a vortex-lattice analysis code (AVL)[‡] with the experiment. The lower inset shows that the present method and AVL show close accord in the effect of ϕ on the lift-curve slope, but with an offset. The AVL prediction for the monoplane was used as $C_{L\alpha\text{-mono}}$ in the present theory [Eq. (9)]. Simulating the body in the AVL predictions leads to an overestimation of the lift-curve slope. Fortuitously, the average of the AVL predictions (with and without body) shows a close match to experiment (not shown). To more closely access the predictive ability of the theory to estimate the impact of nonplanarity, the experimental lift-curve-slope data was reduced by the monoplane lift-curve slope, as presented in the middle inset of Fig. 6. The agreement of Eq. (9) and AVL with experiment is excellent and is particularly encouraging when considering the simplifications required in the theory. The top inset shows the estimated values of e (Eq. (14)) along with AVL's prediction and the experimental lift-curve-slope ratio. As may be expected, agreement is good, considering the results presented in the middle inset. Note that AVL does not indicate that the ratio of the lift-curve slopes is equivalent to e (but is close), as predicated by the present theory (an outcome stemming from its essentially 2-D formulation). Note that determination of experimental e using a linearized drag polar indicates values for the X-wings in the 0.7 range, as opposed to $e > 1$ for all X-wing settings as predicted by theory. The discrepancy is due to the significant viscous effects on the airfoil section and consequent pressure drag. The experimentally determined lift-curve slopes have a reduced impact of viscous effects compared with drag. Note that the theoretical minimum e is 1, as the slender-wing-based formulation used in this paper uses a wake trace for a flat plate and so assumes uniform downwash and thus elliptic loading. Although not explored in this study, roll control could potentially be effected through asymmetric deployment of the wings, as shown in the lower inset of Fig. 1: a design option that may simplify wing design (no ailerons).

Conclusions

An experimental and theoretical investigation was conducted to evaluate the performance of a morphing X-wing configuration. Low-speed wind-tunnels tests showed that the X-wing significantly increases lift compared with the comparative monoplane, and despite a minimum-drag penalty, the endurance parameter $C_L^{3/2}/C_D$ increased markedly. The maximum L/D ratio did not increase relative to the monoplane, due to a large increase in the zero-lift drag coefficient of the X-wing configuration. Comparisons of the developed theory with experiment showed close accord. For the wing configurations tested, a wing dihedral/anhedral angle of 20 to 30 deg showed the best performance. For practical application, the aerodynamic benefits of the X-wing would need to be weighed against this geometry's increase in structural weight and manufacturing complexity.

Acknowledgments

The authors would like to thank the Associate Editor and reviewers for their comments and suggestions.

References

[1] Jha, A. K., and Kudva, J. N., "Morphing Aircraft Concepts, Classifications, and Challenges," *Proceedings of SPIE: The International Society for Optical Engineering*, Vol. 5388, 2004, p. 213.

[‡]Data available online at http://web.mit.edu/drela/Public/web/avl/ [retrieved 10 July 2009].

[2] Bourdin, P., Gatto, A., and Friswell, M. I. "Aircraft Control via Variable Cant-Angle Winglets," *Journal of Aircraft*, Vol. 45, No. 2, 2008, pp. 414–423. doi:10.2514/1.27720
[3] Weisshaar, T. A., "Morphing Aircraft Technology New Shapes for Aircraft Design," NATO Rept. RTO-MP-AVT-141, Oct. 2006.
[4] Lee, D. H., and Weisshaar, T. A., "Aeroelastic Studies on a Folding Wing Configuration," AIAA Paper 2005-1996, April, 2005.
[5] Lowson, M. V., "Minimum Induced Drag for Wings with Spanwise Camber," *Journal of Aircraft*, Vol. 27, No. 7, 1990, pp. 627–631. doi:10.2514/3.25332
[6] Cone, C. D., "The Theory of Induced Lift and Minimum Induced Drag on Non Planar-Lifting Systems," NASA TR-R-139, 1962.
[7] Letcher, J. S., Jr., "V-Wings and Diamond Ring Wings of Minimum Induced Drag," *Journal of Aircraft*, Vol. 9, No. 8, 1972, pp. 605–607. doi:10.2514/3.59045
[8] Smith, J. H. B., "Improved Calculation of Leading Edge Separation from the Slender Delta Wings," Royal Aircraft Establishment, TR 6607, Farnborough, England, U.K., March, 1966.
[9] Jones, R. T., "Properties of Low Aspect Ratio Wings Below and Above the Speed of Sound," NACA Rept. 835, 1946.
[10] Munk, M. M., "Some Tables of the Factor of Apparent Additional Mass," NACA TN 197, July 1924.
[11] Anderson, J., *Aircraft Performance & Design*, 1st ed., McGraw–Hill Science/Engineering/Math, New York, Dec. 1998.